RSC Advances

PAPER

View Article Online
View Journal | View Issue

Cite this: *RSC Adv.*, 2020, **10**, 14915

Double-edged effects and mechanisms of Zn^{2+} microenvironments on osteogenic activity of BMSCs: osteogenic differentiation or apoptosis

Yiqiang Yu, Kai Liu, Zhuo Wen, Weicai Liu, Lei Zhang and Jiansheng Su*

Zinc-incorporated biomaterials show promoting effects on osteogenesis; however, excessive zinc ions lead to cytotoxic reactions and also have other adverse effects. Therefore, the double-edged effects of Zn^{2+} microenvironments on osteogenesis may become critical issues for new material development. This study systematically investigated the bidirectional influences of diverse Zn^{2+} microenvironments on the cell adhesion, proliferation, osteogenic differentiation and apoptosis of rBMSCs. Furthermore, the mechanisms of zinc-induced osteogenic differentiation of rBMSCs and of cell apoptosis induced by high concentration of Zn^{2+} were both discussed in detail. The results indicated that the Zn^{2+} microenvironments of 2 μg mL^{-1} and 5 μg mL^{-1} effectively improved the initial adhesion and proliferation of rBMSCs, while that of 15 μg mL^{-1} had exactly the opposite effect. More importantly, the suitable Zn^{2+} microenvironments (2 μg mL^{-1} and 5 μg mL^{-1}) moderately increased the intracellular Zn^{2+} concentration by regulating zinc transportation, and then activated the MAPK/ERK signaling pathway to induce the osteogenic differentiation of rBMSCs. In contrast, the high Zn^{2+} concentration (15 μg mL^{-1}) not only inhibited the osteogenic differentiation of rBMSCs by damaging intracellular zinc homeostasis, but also induced rBMSC apoptosis by enhancing intracellular ROS generation. The current study clarified the double-edged effects of Zn^{2+} microenvironments on the osteogenic properties of rBMSCs and the related mechanisms, and may provide valuable guidance for optimizing the design of zinc-doped biomaterials and zinc-based alloys.

Received 15th February 2020
Accepted 27th March 2020

DOI: 10.1039/d0ra01465f

rsc.li/rsc-advances

1. Introduction

Currently, rapid bone regeneration and long-term sustained osseointegration are still major challenges for bone regeneration biomaterials and orthopedic implants. In recent years, zinc-containing biomaterials such as metallic zinc alloys,[1] zinc bone cements,[2] bioglasses,[3] hydrogels[4] and coatings[5] have gained extensive attention due to their biocompatibility, osteogenic activity and antibacterial properties, and these effects mainly result from released zinc ions (Zn^{2+}).[6] Zn^{2+} ions are essential cofactors for key enzymes related with bone metabolism (*e.g.* alkaline phosphatase, collagenase, carbonic anhydrase) and are involved in energy metabolism of bone cells.[7] In addition, Zn^{2+} ions show desirable osteogenic activity by stimulating osteoblast proliferation and mineralization,[5,8] and promoting the expression of osteoblast marker genes and collagen secretion of bone marrow mesenchymal stem cells (BMSCs).[5,9,10] However, boon and bane of Zn^{2+} coexist in bone formation. Facilitation on bone regeneration is only one side of Zn^{2+}, while high concentration of Zn^{2+} may lead to cytotoxic reactions and cell apoptosis.[11,12] Considering the long-term exposure of Zn^{2+} microenvironments surrounding zinc-containing biomaterials to bone tissues, their sustained biosecurity and bifunctionality are the key factors determining the clinical application prospects of newly developed materials. Therefore, in order to control and optimize Zn^{2+} microenvironments precisely, it is urgent to comprehensively survey both positive and negative effects of Zn^{2+} microenvironments on osteogenesis and to clarify the involved mechanisms. These issues play important roles to ensure the biosafety and osteoinductivity of materials and have guiding significance for the development of zinc-containing biomaterials.

Although zinc element has great importance in bone metabolism, its biological effects on osteoblasts and MSCs are closely related to Zn^{2+} concentrations. Studies have concluded that zinc exposure in hBMSCs induced osteoblast differentiation and increased mRNA and protein levels of the RUNX2 in a dose-dependent manner.[13] For rat adipose tissue-MSCs (rADSCs), only a specific concentration (0.432 μg mL^{-1}) of zinc sulfate can promote its proliferation.[14] Associated with different zinc contents and Zn^{2+} release kinetics, zinc alloys and zinc-loaded biomaterials could generate various extracellular microenvironments of Zn^{2+} ions showing diverse biological

Department of Prosthodontics, School & Hospital of Stomatology, Tongji University, Shanghai Engineering Research Center of Tooth Restoration and Regeneration, Shanghai 200072, China. E-mail: sjs@tongji.edu.cn; Fax: +86-21-66524025; Tel: +86-21-56722215

effects. Moreover, previous studies demonstrated that zinc ion implantation of titanium,[5] titanium surfaces modified with Zn-incorporated nanotube arrays[10] and zinc-doped metal–organic framework coating[15] exhibited various osteogenic activities with different dose of zinc load and release. More interestingly, the osteogenic effects of these materials did not get synchronous promotion with the increase of their Zn^{2+} contents. Based on these peculiar biological effects of Zn^{2+}, it is crucial to explore the optimized and safe Zn^{2+} microenvironments for osteoinduction and bone formation, further to guide the regulation of zinc loading and release of zinc-incorporated biomaterials, which greatly determine their application prospects. However, what kind of Zn^{2+} microenvironments is most suitable for the growth and osteogenic differentiation of BMSCs remains unknown due to the variety of materials and their respective zinc release characteristics. Besides, the mechanisms of zinc-induced osteogenic differentiation of BMSCs need systematical study.

Appropriate concentrations of Zn^{2+} have certain osteoinductivity, however high concentrations of Zn^{2+} microenvironments may conversely inhibit cell growth and osteogenesis. Uncontrolled rapid release of zinc ions can disrupt intracellular zinc homeostasis and further result in adverse biological effects.[16–20] Although covered by microarc oxidation coating, the undiluted extracts of high-purity zinc exhibited significant cytotoxicity on MG63 cells induced by high concentration of released Zn^{2+}.[17] Besides, it has been reported that Zn^{2+} beyond 400 μM released from zinc-loaded cement induced apoptosis of mouse osteoblasts.[18] In addition, compared with an equal concentration of $ZnCl_2$, released ZnO nanoparticles (ZnO NPs) can give out increased Zn^{2+} and induce more obvious cytotoxicity.[19] In brief, because of the excessive Zn^{2+} release, the biomaterials overloaded with Zn^{2+} or ZnO NPs may have negative biological effects such as cytotoxicity and apoptosis of osteoblast-related cells, while osteocyte apoptosis is exactly a significant factor in skeletal aging and bone resorption.[20] Especially, BMSCs are important precursor cells of osteoblasts and chondroblasts, and their osteogenic differentiation plays a vital role in osteogenesis process. However, the adverse influence of high concentration of Zn^{2+} microenvironments on the growth and osteogenic differentiation of BMSCs and the related mechanisms remain obscure and these problems are critical for the development of zinc-loaded bone regeneration materials.

The biphasic effect of Zn^{2+} on cells is closely related to both extracellular Zn^{2+} microenvironments and intracellular Zn^{2+} concentration. It has been known that maintaining cellular zinc homeostasis greatly depends on bi-directional zinc transport associated with the expression of transmembrane zinc transporters.[21] Among them, the ZnT family (cation diffusion facilitator, SLC30) and ZIP (Zrt- or Irt-like protein, SLC39) family play critical roles.[22] More importantly, recent studies confirmed that zinc-incorporated titanium could regulate cellular zinc transportation by affecting the expressions of the ZnT family and ZIP family.[23,24] Hence, zinc transporters may be the key to clarify the mechanism of dual effects of Zn^{2+} on osteoblast-related cells.

To reveal the bidirectional regulatory function of zinc on osteogenesis, this study comprehensively investigated the adhesion, proliferation and osteogenic differentiation of rBMSCs cultured in various concentrations of Zn^{2+} microenvironments, exploring suitable Zn^{2+} microenvironments that can stimulate the growth and osteogenic differentiation of BMSCs. Furthermore, focused on MAPK/ERK pathway, zinc transporter expression and ROS generation, the underlying mechanisms of zinc-induced osteogenic differentiation and apoptosis of BMSCs were studied. This research may provide valuable references for optimizing the development of zinc-containing bone implants and bone regeneration materials.

2. Materials and methods

2.1 Cell isolation and culture

All animal procedures were performed in accordance with the Guidelines for Care and Use of Laboratory Animals of Tongji University and approved by the Animal Ethics Committee of Hospital of Stomatology affiliated to Tongji University. Rat bone marrow mesenchymal stem cells (rBMSCs) were isolated from femora of 4 week-old Sprague–Dawley (SD) rats as was described.[5] In brief, femoral marrow was extracted and suspended in alpha-minimum essential medium (α-MEM, Hyclone, USA) containing 10% fetal bovine serum (Gibco, USA) and 1% penicillin and streptomycin (Hyclone, USA) at 37 °C in a 5% CO_2 incubator. The medium was refreshed every 3 days. The rBMSCs were grown to 70–80% confluence and then incubated in a 0.25% trypsin/EDTA (Gibco, USA) solution for 1 min at 37 °C to detach the cells. The rBMSCs at the 3–4 passages were used for biological experiments. In order to determine the effects of diverse Zn^{2+} microenvironments on cells, the rBMSCs were culture in four kinds of culture medium with different concentrations of $ZnSO_4$ (Aladdin, China). The experiment was divided into four groups: control group (α-MEM without $ZnSO_4$) and three experimental groups (α-MEM with Zn^{2+} concentrations of 2, 5 and 15 μg mL^{-1} respectively).

2.2 Cell adhesion activity assay

Firstly, rBMSCs (5×10^4 cells per well) were seeded in different concentrations of Zn^{2+} in 24 well plates.[25] After culturing for 1, 4, and 24 h, the cells were washed with the phosphate buffer saline (PBS) for three times, fixed in 4% paraformaldehyde (PFA) for 10 min at room temperature. And then, the cells were permeabilized with 0.1% (v/v) Triton X-100 (Weiao, China) and blocked in bovine serum albumin (Sigma, USA) successively. After rinsing the cells three times with PBS, the cells were stained with fluorescein-isothiocyanate-labeled phalloidin (Sigma, USA) at room temperature in the dark for 30 min. The cells were further counterstained with DAPI (Sigma, USA) for 5 min. The β-actin and cell nuclei were observed with a fluorescence microscope (Carl Zeiss, Germany).

2.3 Cell proliferation measurement

The cell counting kit-8 (CCK-8) assay (Beyotime, China) was performed to evaluate cell proliferation and viability on the

samples. Briefly, rBMSCs were inoculated in the 24-well plates at a density of 1×10^4 per well in various culture medium. After 24 h, the medium was replaced by maintenance or experimental medium containing 2, 5 and 15 μg mL^{-1} Zn^{2+}, with three biological replicates per group. After culturing for 1, 4 and 7 days, the medium was removed and rinsed three times with PBS. The culture medium containing 10% CCK-8 was added to each well and then incubated in dark for another 2 hours. The absorbance at 450 nm was determined by a microplate reader.

2.4 LIVE/DEAD staining

LIVE/DEAD™ Viability/Cytotoxicity Kit (Thermo, USA) was used to analyze qualitative cell viability in order to quickly distinguish living cells from dead ones.[26] In brief, cells were cultured in the 6-well plates at a density of 1×10^5 per well in different culture medium for 24 h as described above. The cells were washed twice with PBS prior to the assay to remove or dilute serum esterase activity. After using sufficient volume of Calcein-AM/EthD-I solution to fully covered cells for 40 minutes, fluorescence microscopy (Carl Zeiss, Germany) was used to observe the images of the viable cells and dead cells.

2.5 ALP staining and ALP activity assay

For the alkaline phosphatase (ALP) staining, the rBMSCs were cultured in 24-well plates for each group. After being incubated for 7 and 14 days, the cells were fixed with PFA for 30 min and then rinsed three times with PBS. The cells were added an appropriate amount of BCIP/NBT staining work-fluid (Beyotime, China) to ensure fully covered cells for 30 minutes. For ALP activity assay, rBMSCs were incubated with *p*-nitrophenyl phosphate (*p*NPP) (Jiancheng, China) at 37 °C for 30 min. ALP activity was determined by detecting optical density (OD) values at 405 nm. The content of total protein was extracted by BCA protein assay kit (Beyotime, China) and measured according to the manufacturer's instructions. ALP activity was normalized to the total protein content as previously described.[27]

2.6 Real-time quantitative polymerase chain reaction analysis

The rBMSCs were cultured in 6-well plates in different culture medium for 3 and 10 days, respectively. Total RNA was isolated using 800 μL TRIZOL reagent (Takara, Japan) and 1.0 mg RNA was reversed transcribed to cDNA using PrimeScript RT Master Mix (Takara, Japan) according to the manufacturer's instructions. Gene expression was quantified by using Universal SYBR Green Master (Roche, USA). The expression of these genes, including integrin α1, integrin β1, Col-1, ALP, OPN, ZIP1 and ZnT1 was assayed respectively. Real-time PCR assay was repeated three times for each group. The gene expression level of each target gene was calculated by the $\Delta\Delta C_T$ method and was normalized to that of the reference gene GAPDH.[24] The primers sequences for the selected genes were shown in Table 1.

2.7 Intracellular zinc ions detection

To detect the concentrations of intracellular Zn^{2+}, the rBMSCs (1×10^4 cells per mL) were cultured on cell culture dish (∅100 mm) for 12 days.[23] After being centrifuged with 0.25% trypsin/EDTA, the cells were resuspended three times with physiological saline and counted under a light microscope. The concentrations of Zn^{2+} in rBMSCs were measured with an inductively coupled plasma mass spectrometry (ICP-MS, Thermo, USA).

2.8 Western blot

The rBMSCs were cultured in different culture medium for 3 days. For total protein extraction, rBMSCs were lysed in ice-cold RIPA buffer and centrifugated at 12 000 rpm for 10 min at 4 °C.[28] The amount of proteins was quantified using a BCA protein assay kit (Beyotime, China). By sodium dodecyl sulfate polyacrylamide gel electrophoresis (SDS-PAGE, Epizyme, China), the protein samples (10 μg) were separated and transferred to 0.22 μm pore-sized poly-vinylidene difluoride membranes (PVDF, Sangon, China). After being blocked with 0.1% tween containing 5% nonfat dry milk solution for 1 h at room temperature, the membranes were incubated overnight at 4 °C with anti-p-ERK1/2, ERK1/2 (1 : 1000, Abcam, UK), anti-RUNX-2 (1 : 1000, CST, USA), anti-GAPDH (1 : 1000, Boster, China) in the blocking buffer. After being incubated with the secondary antibodies for 1 h, specific protein bands were detected using an enhanced chemiluminescence detection system (Millipore, USA). For western blot analysis, GAPDH protein expression was used as an endogenous control for normalization.[29]

2.9 Intracellular reactive oxygen species measurement

Reactive oxygen species (ROS) production was measured by the dichlorofluorescein diacetate (DCFH-DA) cellular ROS detection assay kit (Beyotime, China). The rBMSCs (1×10^5 cells per mL on 6-well plates) were treated with different concentrations of Zn^{2+} for 24 h. The cells were incubated with 10 μM DCFH-DA at 37 °C in the dark for 30 min, which oxidized into fluorescent DCF in the presence of ROS, and then washed three times using PBS. Images were obtained using a fluorescence microscope (Carl Zeiss, Germany). The intracellular ROS production were analyzed using ImageJ software according to the numbers of ROS-positive BMSCs in the images of each group as previously described.[29] Then the ratio of ROS-positive BMSCs numbers of each group to those of control group was calculated and expressed as ratio of ROS (+) cell numbers to control. Beyond that, the harvested cells were collected and analyzed by a flow cytometry (Thermo, USA). The data were acquired and analyzed with FlowJo10.0 software (TreeStar Inc., OR, USA). The relative ratio of ROS generation in each experimental group to that in control group was expressed as fold change of ROS generation to control.

2.10 Cell apoptosis assay

Apoptotic cells were identified using a Fluorescein Isothiocyanate (FITC)-Annexin V/Propidium Iodide (PI) Apoptosis Kit[30] (BD Biosciences, USA). Briefly, 1×10^6 cells were treated

Table 1 Primer sequences used for real-time PCR

Gene	Species	Forward primer sequence (5′–3′)	Reverse primer sequence (5′–3′)
GAPDH	Rat	GGCAAGTTCAACGGCACAGT	GCCAGTAGACTCCACGACAT
Integrin α1	Rat	AGCTGGACATAGTCATCGTC	AGTTGTCATGCGATTCTCCG
Integrin β1	Rat	AATGTTTCAGTGCAGAGCC	TTGGGATGATGTCGGGAC
Col-1	Rat	CGTGACCTCAAGATGTGCCA	TCGATCCAGTACTCTCCGCT
ALP	Rat	CGGAAGTGAGGCAGGTAG	AGAGCCCACAATGGACAG
OPN	Rat	TGGATGAACCAAGCGTGGA	TCGCCTGACTGTCGATAGCA
ZIP1	Rat	GCGTGCCTGTGTACTGGTCTTC	CGCTCGTAGGTGGCTCTGTAGA
ZnT1	Rat	AGGCAGAGAAGGCTCCAACAGT	TGTGCGACCAGACGAGGACTT

with different concentrations of Zn^{2+} for 24 h. After treatment, the cells were washed twice with cold PBS and then resuspend cells in 300 μL 1× binding buffer into a sterile flow cytometry glass tube. Annexin V (10 μL) was added to the glass tube and incubated for 15 min at room temperature in the dark, meanwhile gently vertexing the cells. After being treated with 5 μL PI, the cells were incubated at room temperature for 5 min in the dark. Following incubation, the percentage of apoptotic and necrotic cells were analyzed using flow cytometry (Thermo, USA).

2.11 SEM examination

For SEM examination, rBMSCs (2×10^5 cells per well) were seeded in 24 well plates with various culture medium. After 24 h of cell culture, the cells were rinsed with PBS, fixed with 2.5% glutaraldehyde solution and dehydrated with a series of graded ethanol/water solutions. After being coated with platinum, the samples with cells were observed with a scanning electron microscopy (SEM, Hitachi S4800, Japan) as previously described.[31]

2.12 Statistical analysis

All data are expressed as mean ± standard deviation (SD) at least three independent experiments. Statistical analyses were determined by one-way ANOVA tests with $*p < 0.05$ and $**p < 0.01$ considered statistically significant and were performed using GraphPad Prism5.0.

3. Results and discussion

3.1 Bidirectional influences of Zn^{2+} microenvironments on cell adhesion and spreading of rBMSCs

BMSCs, the precursor of osteoblasts, play a significant role in bone regeneration and osseointegration, and the rapid recruitment and adhesion of BMSCs are the initial stages of bone formation. Furthermore, cell adhesion can affect the proliferation, differentiation and mineralization of osteoblasts.[32] Previous studies have shown that both zinc ion implanted titanium and titania nanotubes incorporated with zinc can promote rBMSCs adhesion.[10,23] However, the optimal zinc ion microenvironments conducive to cell adhesion and spreading, and especially the related mechanisms remain obscure. Therefore, the influences of various concentrations of Zn^{2+} microenvironments on initial adhesion and spreading of rBMSCs were visualized using fluorescent staining images. After rBMSCs being seeded for 4 h and 24 h, compared with the control group, an increased cell density and better cell spreading morphology with more obvious filopodia extension were shown clearly in Zn^{2+} microenvironments of 2 μg mL^{-1} and 5 μg mL^{-1}, while in that of 15 μg mL^{-1}, much less adherent rBMSCs with limited filopodia extension occurred (Fig. 1A). These results suggested that Zn^{2+} microenvironments of 2–5 μg mL^{-1} effectively promoted cell adhesion and spreading of rBMSCs, which were significantly inhibited in those of 15 μg mL^{-1} instead.

Accordingly, it can be inferred that the adhesion activity of rBMSCs was influenced bidirectionally by the concentrations of Zn^{2+} microenvironments to which the response of rBMSCs exhibited high sensitivity. Recent studies also demonstrated a dose-dependent effect of zinc on cell spreading and adhesion.[5,10] Zinc alloy implants have been found to inhibit cell attachment and viability *in vitro* conditions for fast degradation.[33] In addition, it was reported that both cellular adhesion and cell mobility of human vascular cells may be hindered by high concentration of free Zn^{2+}.[34] However, the dynamic influences of varied zinc microenvironments on the BMSCs adhesion have not been clarified so far. Our data confirmed that the Zn^{2+} microenvironments of 2–5 μg mL^{-1} were optimal for rBMSCs adhesion and spreading, while that of 15 μg mL^{-1} showed inhibitory effect on cell adhesion.

Cellular initial adhesion depends largely on integrins, a kind of transmembrane proteins, which provides critical connection between cells and extracellular environment.[35] Former researches indicated that biomaterials containing zinc and manganese can promote the initial adhesion of BMSCs by up-regulating the expression of integrins.[23,36] Hence, we further investigated the effects of different Zn^{2+} microenvironments on integrin gene expression of BMSCs. The results of real-time PCR analysis showed that, compared to the control group, Zn^{2+} concentrations of 2 μg mL^{-1} and 5 μg mL^{-1} effectively promoted the gene expression of integer α1 and integrin β1 of rBMSCs, while in the group of 15 μg mL^{-1} the expression of these genes was significantly inhibited (Fig. 1B and C). Therefore, it may be inferred that suitable concentrations (2–5 μg mL^{-1}) of Zn^{2+} microenvironments can enhance adhesion activity of rBMSCs by up-regulating the expression of integrins, while an excessively high concentration of Zn^{2+} may

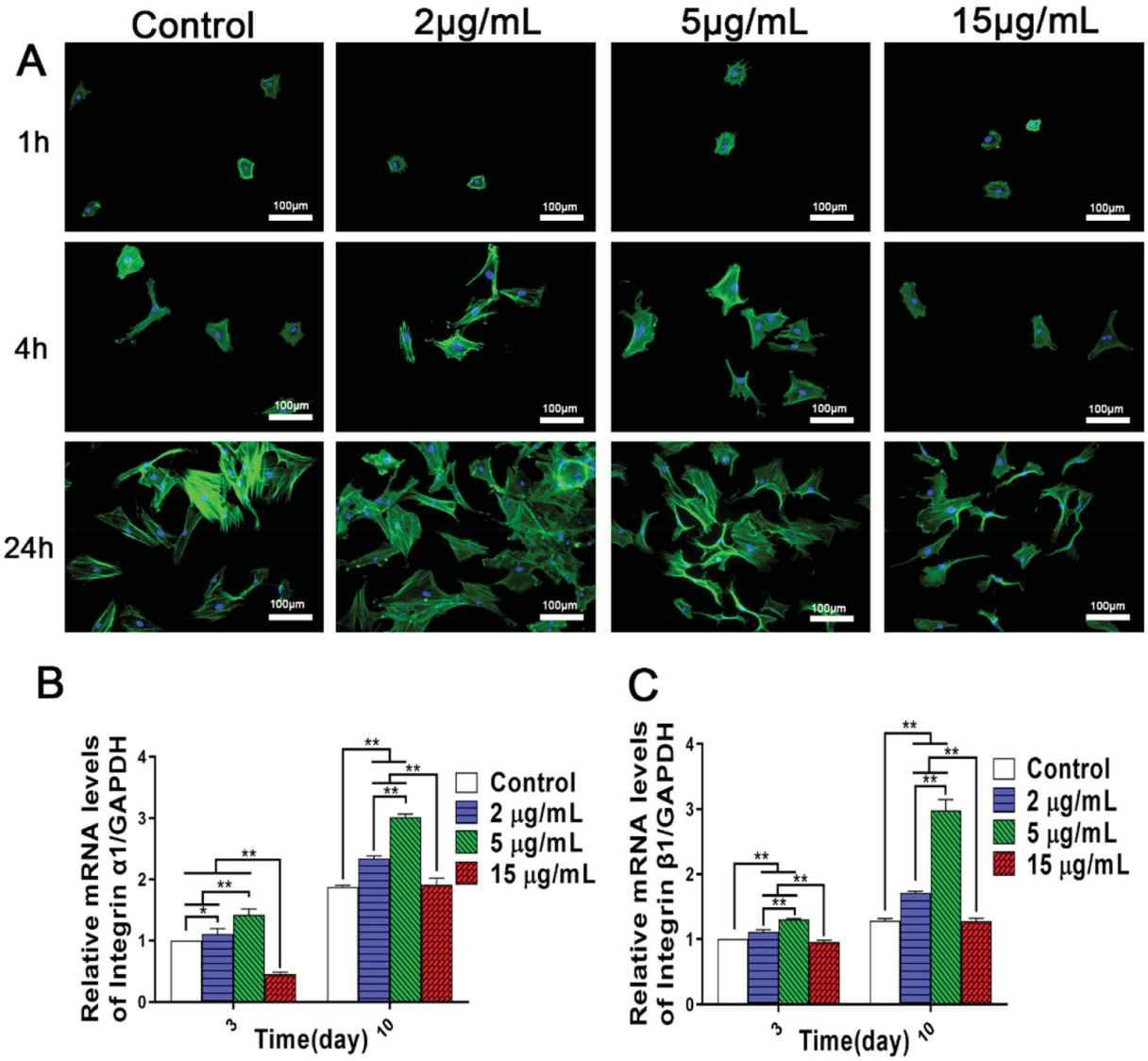

Fig. 1 Bidirectional influences of Zn^{2+} microenvironments on cell adhesion and spreading of rBMSCs. (A) Fluorescent images of rBMSCs cultured in the different concentrations of Zn^{2+} microenvironments for 1, 4 and 24 hours ($n = 3$). (B) Integrin α1 and (C) integrin β1 gene expression of rBMSCs cultured for 3 and 10 days ($n = 3$). The results were normalized to GAPDH and expressed as fold increase relative to control group values. (*) $p < 0.05$, (**) $p < 0.01$.

result in an opposite effect. Previous studies have confirmed that the surfaces of zinc-doped titanium and pure zinc (99.9998%) facilitate BMSCs adhesion,[37,38] and these effects may also be attributed to their released Zn^{2+} that create suitable extracellular microenvironments. The present study not only revealed the appropriate concentration range of Zn^{2+} microenvironments for BMSCs adhesion, but also clarified the underlying mechanism involved.

3.2 Double-edged effects of Zn^{2+} microenvironments on rBMSCs viability and proliferation

The viability and proliferative capacity of BMSCs and osteoblasts play important roles in the process of bone tissue regeneration and osseointegration. Lots of studies showed that zinc ions released from biomaterials can effectively promote the colonization and proliferation of BMSCs and osteoblasts.[3,5,24] However, there were few systematical researches on the relationships between BMSCs proliferation and varied Zn^{2+} microenvironments.

Fluorescent staining images of living/dead cells showed clearly the viability status of rBMSCs cultured in different Zn^{2+} microenvironments. There were much more green-stained living rBMSCs in the groups of 2 μg mL^{-1} and 5 μg mL^{-1} than those in the other two groups. However, the red-stained dead cells were increased significantly in Zn^{2+} concentration of 15 μg mL^{-1} compared to the other groups (Fig. 2A). These interesting phenomena suggest that the Zn^{2+} microenvironments of 2–5 μg mL^{-1} are more beneficial to the viability and growth of rBMSCs, while that of 15 μg mL^{-1} shows some cytotoxicity. Furthermore, the results of quantitative analysis using

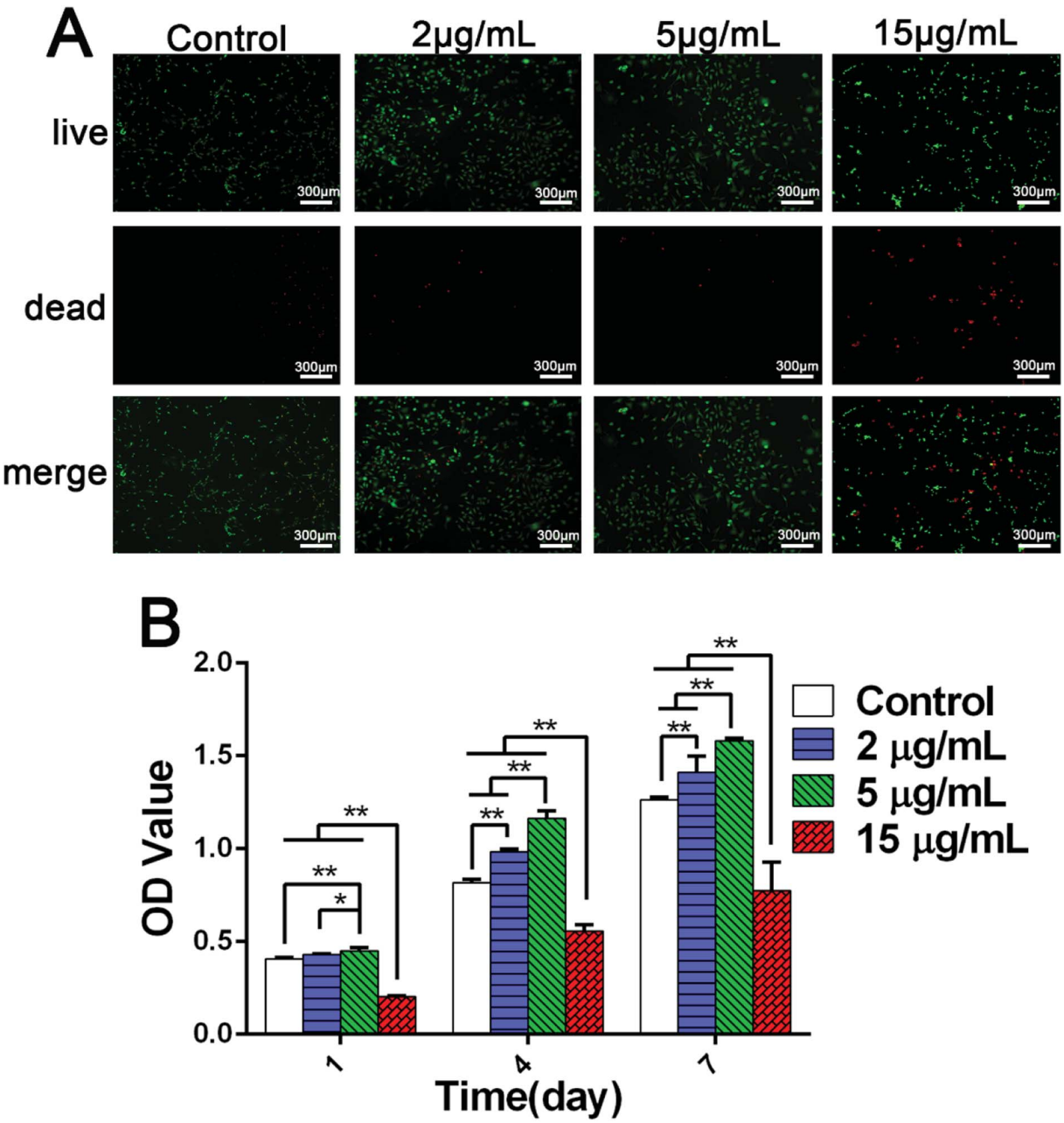

Fig. 2 Double-edged effects of diverse Zn^{2+} microenvironments on cell viability and proliferation of rBMSCs. (A) Fluorescent staining images of living/dead rBMSCs after cultured for 24 h in diverse Zn^{2+} microenvironments. (B) Cell proliferation of rBMSCs cultured for 1, 4 and 7 days. $n = 3$, (*) $p < 0.05$, (**) $p < 0.01$.

CCK-8 assay showed that, after being cultured for 1, 4 and 7 days, the proliferative activity of rBMSCs in groups of 2 μg mL^{-1} and 5 μg mL^{-1} was significantly higher than that of the other two groups ($p < 0.01$), with the most cell number in the group of 5 μg mL^{-1}. On the contrary, the cell proliferation in the group 15 μg mL^{-1} was much lower than those in the other three groups ($p < 0.01$) (Fig. 2B). In short, the above-mentioned results indicated that different Zn^{2+} microenvironments may result in double-edged effects on rBMSCs viability and proliferation. That is, on the one side, the Zn^{2+} microenvironments with appropriate concentrations (2–5 μg mL^{-1}) could promote the proliferation of rBMSCs quickly and effectively, and that of 5 μg mL^{-1} had an optimal effect. On the other side, the proliferation of rBMSCs was greatly inhibited when cultured in Zn^{2+} concentrations beyond 15 μg mL^{-1}.

Studies also confirmed that the effect of zinc on cell proliferation showed a concentration-dependent manner. Conforming to our results, it was reported that Zn^{2+} concentration of 25 μM (1.6 μg mL^{-1}) promoted the proliferation of MC3T3-E1 cells,[39] but $ZnSO_4$ concentration of 200 μM (Zn^{2+} 13 μg mL^{-1}) inhibited the proliferation of hBMSCs.[13] Therefore, only the Zn^{2+} microenvironments with appropriate concentrations can

promote cell proliferation of osteoblast and BMSCs, with too low concentration of Zn^{2+} having no biological effects and too high concentration inducing cytotoxicity. Recent studies have indicated that zinc-loaded biomaterials also have a concentration-dependent effect on cell proliferation. The osteogenic capability of different zinc-incorporated titanium surfaces prepared by means of plasma immersion ion implantation (PIII) and plasma electrolytic oxidation were investigated. Although all the zinc-incorporated materials were found to stimulate proliferation of rBMSCs, it is interesting to note that their promotion effect did not correlate well with the release amount of Zn^{2+}. In fact, the least Zn^{2+} released from Z0-PIII-Zn titanium among these zinc-incorporated coatings resulted in the biggest proliferation rate.[24] Thus, it is quite necessary to strictly control the loading and release quantity of Zn^{2+} during the development of bone regeneration biomaterials. This finding of the study not only clarified the dual effects of Zn^{2+} microenvironments on BMSCs growth but also provided a scientific reference on reasonable Zn^{2+} concentration for the design of zinc-containing materials.

3.3 Positive and negative regulation of Zn^{2+} microenvironments on osteogenic differentiation of rBMSCs

BMSCs have multiple differentiation potential, whose osteogenic differentiation is a vital stage in the process of bone formation.[40] Since we have found that the Zn^{2+} microenvironments have bidirectional regulatory effects on BMSCs adhesion and proliferation, it is more urgent to study how Zn^{2+} microenvironments regulate the osteogenic differentiation of BMSCs. ALP activity and the expression of osteoblast-related genes are highly significant standards to evaluate the osteogenic differentiation of BMSCs. Therefore, the influence of various Zn^{2+} microenvironments on the two indexes were focused on in the present study.

Firstly, the results of ALP assay showed clearly that the intensity of ALP staining and ALP activity in the groups of 2 μg mL^{-1} and 5 μg mL^{-1} were significantly higher than those observed in the control group ($p < 0.01$), especially in the group of 2 μg mL^{-1}. On the contrary, the corresponding results in the group of 15 μg mL^{-1} were much lower compared with the other groups ($p < 0.01$) (Fig. 3A and B). Furthermore, the results of real-time PCR analysis indicated that mRNA expression levels of main osteoblast markers (ALP, Col-1 and OPN) were remarkably up-regulated in the Zn^{2+} microenvironments of 2–5 μg mL^{-1}, while Zn^{2+} microenvironments of 15 μg mL^{-1} evidently suppressed the expression of these genes (Fig. 3C–E). Interestingly, Zn^{2+} microenvironments of 5 μg mL^{-1} up-regulated the gene expression of ALP rapidly at day 3, and the promoting effect was weakened at day 10 (Fig. 3E). ALP activity showed the active function of ALP protein and may not change synchronously with the gene expression of ALP. As a result, ALP activity in group 2 μg mL^{-1} was slightly higher than that in group 5 μg mL^{-1} (Fig. 3B). In brief, it can be inferred that the appropriate concentrations (2–5 μg mL^{-1}) of Zn^{2+} can set up suitable microenvironments for inducing the osteogenic differentiation of BMSCs. Conversely, high concentration of Zn^{2+} over 15 μg mL^{-1} may inhibit the osteoblast differentiation.

These interesting results suggest that osteogenic differentiation of BMSCs needs to be stimulated and induced in specific zinc ion microenvironments. Prior studies have also found that zinc-loaded biomaterials induced osteogenic differentiation of BMSCs in some extent, but their clinical application prospect largely hinged on the amount of incorporated zinc and subsequent optimized release of Zn^{2+} to stimulate osteogenesis or osseointegration.[24,41] For example, despite less Zn^{2+} load and release, the Zn-implanted sub-surface coatings showed much higher osteogenic activity compared to the "bulk-doped" coatings prepared by plasma electrolyte oxidation (PEO).[24] In addition, the promotion effect of zinc-containing bioactive glass on calcified matrix deposition was dose-dependent with low doses of zinc load, with ultrahigh doses of Zn^{2+} inducing reactive oxygen species and cytotoxicity.[8] In fact, on the surface of the polydopamine-immobilized Ti, excessive Cu and Ag produced much more ROS than the negative control and remarkably reduced the osteogenic differentiation of hBMSCs.[42] All these studies and our research suggest that it is essential to strictly control the load and release of Zn^{2+} in developing zinc-incorporated biomaterials, and we also reveal the appropriate Zn^{2+} microenvironments beneficial to BMSC osteogenic differentiation.

From the above-mentioned results, it may be concluded that Zn^{2+} ions have double-edged effects on the osteogenic activity of BMSCs. In order to produce their positive biological effects as far as possible, it is urgent to deeply explore the mechanism on dual regulation of Zn^{2+} microenvironments on BMSCs. Indeed, extracellular Zn^{2+} do not have immediate impact on the osteogenic activity of BMSCs. In fact, they need to be taken into cells by transmembrane zinc transporters on cell surface and need to be accumulated to a certain concentration before they produce physiological effects on cells.[24] It is these transmembrane zinc transporters that regulate intracellular Zn^{2+} content and zinc homeostasis. Among them, ZIP (Zrt- or Irt-like protein, SLC39) family is the main transporters for zinc influx, which is responsible for taking extracellular Zn^{2+} into cells. On the contrary, zinc transporters of the ZnT (cation diffusion facilitator, SLC30) family are ubiquitous zinc exporters which decrease cytoplasmic zinc.[43] Therefore, the ultimate intracellular Zn^{2+} concentration is regulated by the two means. More interestingly, during the osteogenic differentiation process of pluripotent MSCs into osteoblasts, the expression of the ZIP1 protein and zinc uptake were found both increased.[15] Hence, bidirectional transportation of zinc may play a critical role in the osteogenic differentiation of BMSCs.

To clarify the mechanisms on dual regulation of Zn^{2+} on BMSCs, this study further focused on the expression of zinc transporters in BMSCs and intracellular concentration of Zn^{2+}. Firstly, the results of PCR analysis showed that, compared with the control group, the gene expression of ZIP1 and ZnT1 were both up-regulated to a certain extent in Zn^{2+} microenvironments of 2–5 μg mL^{-1}. Meanwhile, the higher concentration of Zn^{2+} (15 μg mL^{-1}) greatly promoted the gene expression of ZIP1, but only increased the expression of ZnT1 slightly (Fig. 4A and

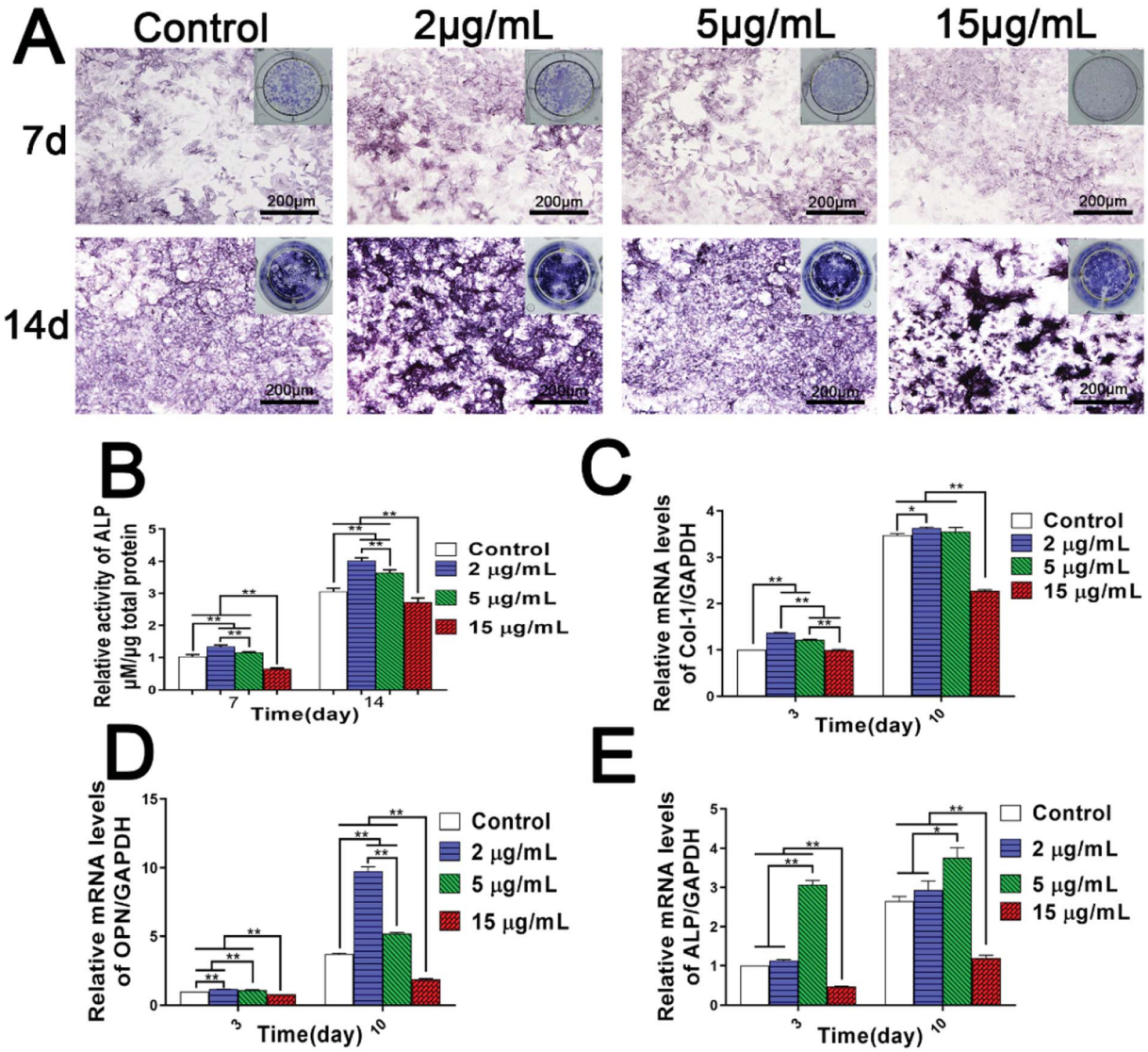

Fig. 3 Dual regulation of Zn^{2+} microenvironments on the osteogenic differentiation of rBMSCs. (A) ALP staining and (B) ALP activity of rBMSCs incubated in various Zn^{2+} microenvironments for 7 and 14 days. $n = 3$. ALP activity was normalized against the total protein concentration measured by a BCA protein assay kit. (C–E) The genes expression of osteoblast markers in rBMSCs cultured in diverse Zn^{2+} microenvironments for 3 and 10 days: (C) Col-1, (D) OPN, (E) ALP. The results were normalized to GAPDH and expressed as fold increase relative to control group values. (*) $p < 0.05$, (**) $p < 0.01$.

B). These interesting results revealed that with the increase of extracellular Zn^{2+} concentration, the zinc inflow in rBMSCs was largely enhanced, while zinc outflow was only increased slightly. Subsequently, the intracellular Zn^{2+} concentrations of rBMSCs were measured using ICP. It was shown clearly that the intracellular concentration of Zn^{2+} also gradually rose with the increase of extracellular Zn^{2+} concentrations (Fig. 4C). All these results suggested that the comprehensive regulation of low concentrations (2–5 μg mL^{-1}) of Zn^{2+} microenvironments on zinc transport resulted in an appropriate increase of the intracellular Zn^{2+} concentration. However, the high concentration (15 μg mL^{-1}) of Zn^{2+} broke the balance of bi-directional zinc transport and led to excessive intracellular zinc ions. In summary, it can be concluded that zinc microenvironments have impact on the zinc transportation of rBMSCs and further regulate Zn^{2+} concentration in cells, thereby influencing the osteogenic differentiation of cells.

Since the zinc microenvironments can regulate the osteogenic differentiation of rBMSCs, it is possible to promote the osteogenic activity of biomaterials by optimizing the doping content and release rate of Zn^{2+}. Our previous research revealed that zinc ion implanted titanium and zinc/magnesium co-implanted titanium can appropriately increase the intracellular Zn^{2+} content by enhancing the expression of ZIP, thereby inducing osteogenic differentiation of rBMSCs.[23] In addition, zinc implanted titanium exhibited better osteogenic activity than PEO titanium, although its promoting effects on Zn^{2+} release and ZIP expression were not as significant as those of PEO titanium.[24] These interesting findings well coincided with the results of the present study. Therefore, it is reasonable to

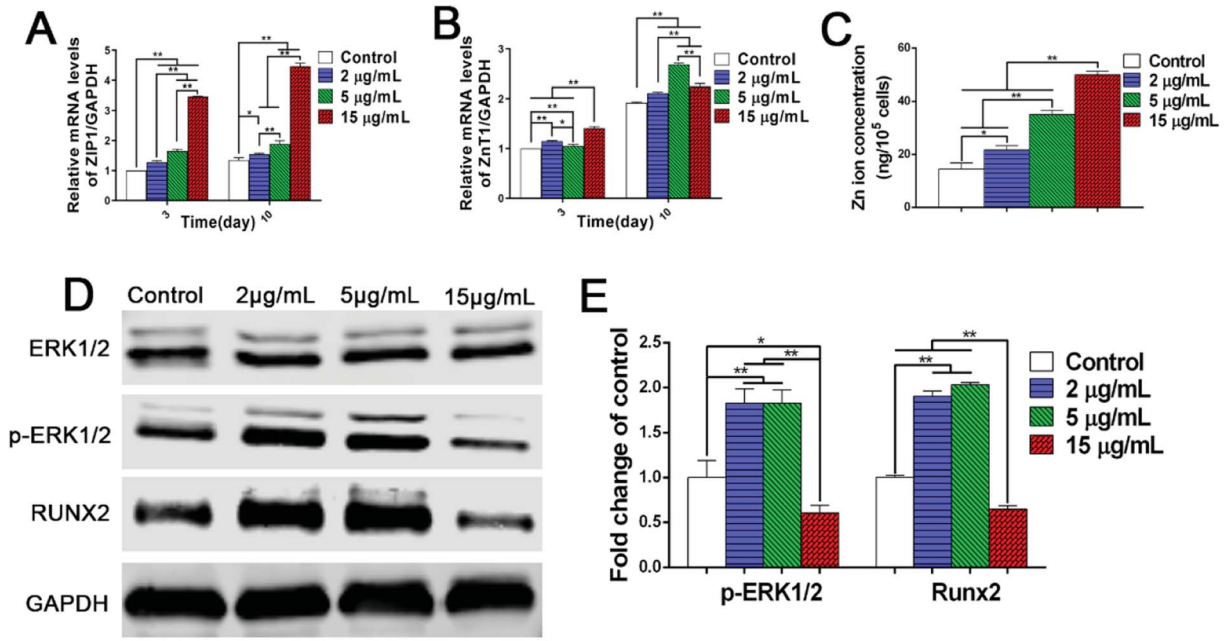

Fig. 4 Involved mechanisms on the dual regulation of Zn^{2+} microenvironments on rBMSCs. (A) ZIP1 and (B) ZnT1 gene expression of rBMSCs cultured in different Zn^{2+} microenvironments for 3 days and 10 days ($n = 3$). (C) Zn^{2+} ions concentrations in rBMSCs cultured in diverse Zn^{2+} microenvironments for 12 days ($n = 3$). (D) Expression profile of key proteins in rBMSCs in the ERK1/2 signaling pathway. (E) Semi-quantitative analysis of the expression of p-ERK1/2 and RUNX2. The band intensities corresponding to p-ERK1/2 and RUNX2 were quantified and normalized relative to that of GAPDH and converted to fold change of control. (*) $p < 0.05$, (**) $p < 0.01$.

conclude that suitable zinc microenvironments (2–5 μg mL^{-1}) can moderately increase intracellular zinc concentration by appropriate up-regulation of ZIP expression, thus inducing osteogenic differentiation of rBMSCs. On the contrary, high concentration (15 μg mL^{-1}) of Zn^{2+} leads to excessive zinc content in BMSCs and inhibits osteogenic differentiation. These significant discoveries can provide scientific reference for the development and clinical application of zinc-doped biomaterials.

The transcription of genes is only involved in the initial stage of protein synthesis, while the functional proteins translated from mRNA are the keys to physiological functions. Since zinc microenvironments have the ability to influence the expression of osteogenesis-related genes (Fig. 3C–E), it is necessary to further explore the protein signaling pathway in osteogenic differentiation induced by zinc ions. As shown in western blot images, Zn^{2+} microenvironments of 2–5 μg mL^{-1} induced the phosphorylation of extracellular signal-related kinases (ERK) 1/2 protein shown as the up-regulated expression level of p-ERK1/2 protein, and further promoted the expression of downstream RUNX2 (runt-related transcription factor 2) protein (Fig. 4D and E). In contrast, the high concentration (15 μg mL^{-1}) of Zn^{2+} inhibited the phosphorylation of ERK1/2 protein and RUNX2 protein expression (Fig. 4D and E). These results well explained the bidirectional regulation of Zn^{2+} microenvironments on osteogenic differentiation of BMSCs. Several previous studies also found that the osteogenic capacity of BMSCs could be promoted by either mineral trioxide aggregate or calcium silicate bioglass *via* MAPK/ERK signaling pathway.[27,44] Furthermore, the downstream RUNX2 protein was found to play an important role both in the osteogenesis process and the MAPK signaling pathway.[45,46] Also, it has been proved that zinc exerts osteogenic effects on hBMSCs by increasing mRNA and protein levels of the master transcriptional factor RUNX2.[13] In conclusion, it can be inferred that the appropriate Zn^{2+} microenvironments (2–5 μg mL^{-1}) induce the osteogenic differentiation of rBMSCs by activating the MAPK/ERK signaling pathway; while higher concentration (15 μg mL^{-1}) of Zn^{2+} inhibits that signaling pathway and osteogenic differentiation. These findings may clarify the underlying mechanism on osteogenic differentiation regulated by diverse Zn^{2+} microenvironments in both positive and negative aspects.

3.4 rBMSCs apoptosis induced by high concentration of Zn^{2+} microenvironments

With the *in vivo* degradation of zinc alloys and zinc doped implants, zinc ions are released continuously and accumulated in the local microenvironments surrounding bone implants. However, rapid release of Zn^{2+} may lead to a high concentration of zinc in local bone tissue and cause adverse effects on cell growth and bone regeneration. It was reported that Zn^{2+} induced cell apoptosis of mouse fibroblasts NIH3T3 and mouse osteoblasts when the concentrations reached 70 μM and 400 μM respectively.[18,47] In addition, iron overload damaged the endothelial mitochondria *via* the ROS/ADMA/DDAHII/eNOS/NO pathway.[48] However, the influence of excessive Zn^{2+} ions on the apoptosis of BMSCs and the involved mechanism still remain obscure. These issues are the crucial factors to explore

the negative effects of zinc microenvironments on the growth and osteogenic activity of BMSCs.

Unlike cell necrosis, cell apoptosis is an autonomic programmed cell death controlled by genes. Apoptosis of rBMSCs is not necessarily caused by cytotoxicity, but is closely related to intracellular ROS production. Recently, it has been demonstrated that overloaded metal ions such as iron can trigger oxidative stress by increasing reactive oxygen species (ROS) and participate in apoptosis and pyroptosis,[49] showing that ROS may play a vital role in metal ion-induced apoptosis. Therefore, the influence of Zn^{2+} microenvironments on ROS generation in rBMSCs was analyzed firstly. The results of fluorescence staining and flow cytometry analysis confirmed consistently that the amount of intracellular ROS production in rBMSCs rose synchronously with the increase of Zn^{2+} concentration (Fig. 5A and B). It was reported that excessive metal ions such as Cu and Ag also produced increased ROS and significantly inhibited osteogenic activity of hBMSCs.[42] Therefore, the increased ROS generation in rBMSCs well explained the negative effect of high concentration of Zn^{2+} ions on osteogenic differentiation of rBMSCs.

Furthermore, the effects of Zn^{2+} microenvironments on the apoptosis of rBMSCs were investigated using flow cytometer. The results showed that the apoptosis rate of rBMSCs in the group of 15 μg mL^{-1} was much higher than other groups ($p < 0.01$), with no statistical differences existing between the other three groups (Fig. 5C). In addition, SEM images revealed the rBMSCs apoptosis induced by high concentration of Zn^{2+} from the aspect of cell morphology. Being cultured in the Zn^{2+} microenvironments of 5 μg mL^{-1}, the rBMSCs showed healthy growth morphology and obvious filopodia extension (Fig. 6A and C). In contrast, under the high concentration (15 μg mL^{-1}) of Zn^{2+}, the majority of cells exhibited shrunk morphology with reduced volume (Fig. 6B). The typical apoptotic cell morphology, with poor cell spreading and filopodia disappearance, was shown in the high magnification (Fig. 6D). These phenomena comply with the apoptotic morphological character reported in previous studies.[31] In short, all the above results consistently demonstrate that the Zn^{2+} microenvironments of 15 μg mL^{-1} can significantly induce BMSCs apoptosis by promoting their intracellular ROS generation, while those of 2–5 μg mL^{-1} do not induce apoptosis. A recent research showed that oxidative stress increased BMSC apoptosis and impaired mitochondrial potential by promoting ROS synthesis and further inhibited proliferation, migration and paracrine of BMSC which were very important for bone reconstruction.[50] Similarly, the results of our study revealed that the high concentration (15 μg mL^{-1}) of Zn^{2+}, which was not conducive to osteogenesis, increased ROS generation and then impaired the adhesion, proliferation and osteogenic differentiation of rBMSCs.

Similar to excessive Zn^{2+} ions, negative effects also occured in nano-sized zinc oxide (Nano-ZnO). ZnO-NPs can rapidly release zinc ions due to their ultra-fine size and high specific

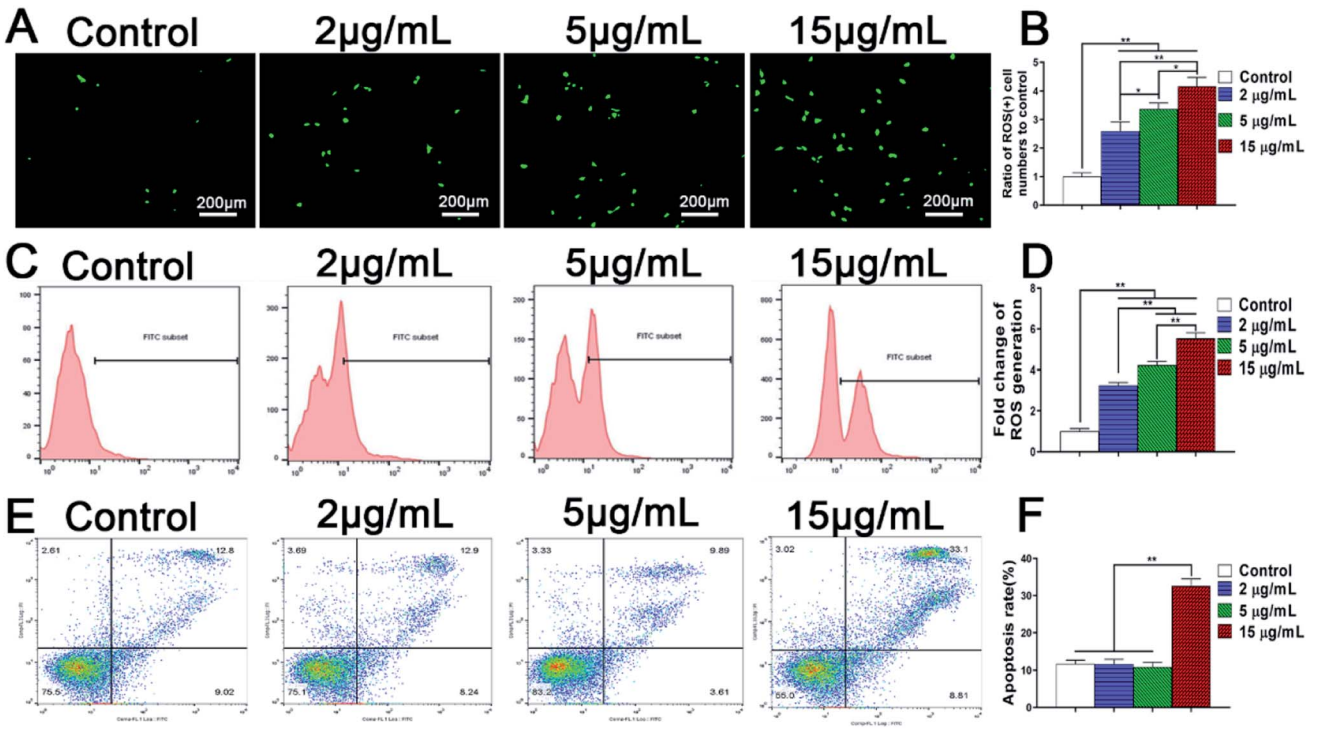

Fig. 5 ROS generation and apoptosis of rBMSCs cultured in different Zn^{2+} microenvironments for 24 h. (A) Fluorescent staining images of ROS-positive rBMSCs *via* DCFH-DA staining; (B) ratio of ROS (+) cell numbers to control referred to the ratio of ROS-positive BMSCs numbers of each group to those of control group; (C) flow cytometric analysis of ROS-positive cells stained by DCFH-DA; (D) fold change of ROS generation referred to the relative ratio of ROS generation in each experimental group to that in control group; (E) flow cytometry measurement of apoptosis, rBMSCs were stained with annexin V-FITC/PI; (F) cell apoptosis rate of rBMSCs. (*) $p < 0.05$, (**) $p < 0.01$.

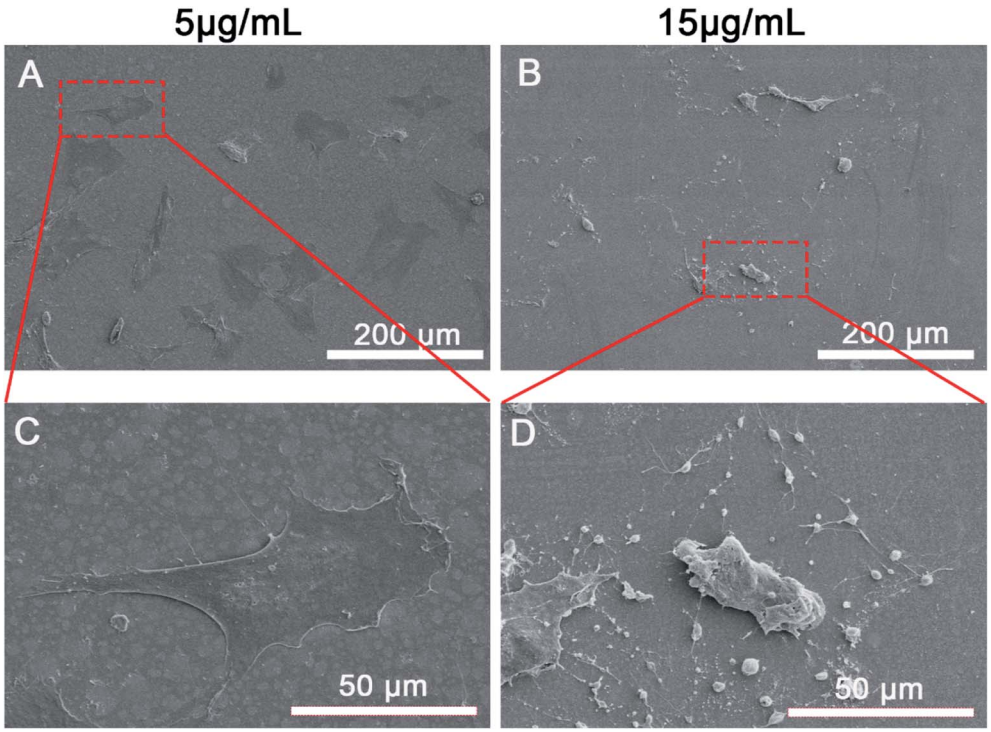

Fig. 6 SEM images of the morphology of rBMSCs cultured in Zn^{2+} microenvironments of (A) 5 μg mL^{-1} and (B) 15 μg mL^{-1}. (C and D) Partial magnifications of the rectangular regions in the upper corresponding SEM images.

surface area.[51] Besides, the excessive exposure of ZnO-NPs was found to interfere with the intracellular homeostasis of zinc and lead to cell apoptosis.[52] In recent years, Nano-ZnO was confirmed to own the property of inducing an excessive production of ROS which then activated the apoptosis pathway mediated by mitochondria and caspases.[53] In addition, many

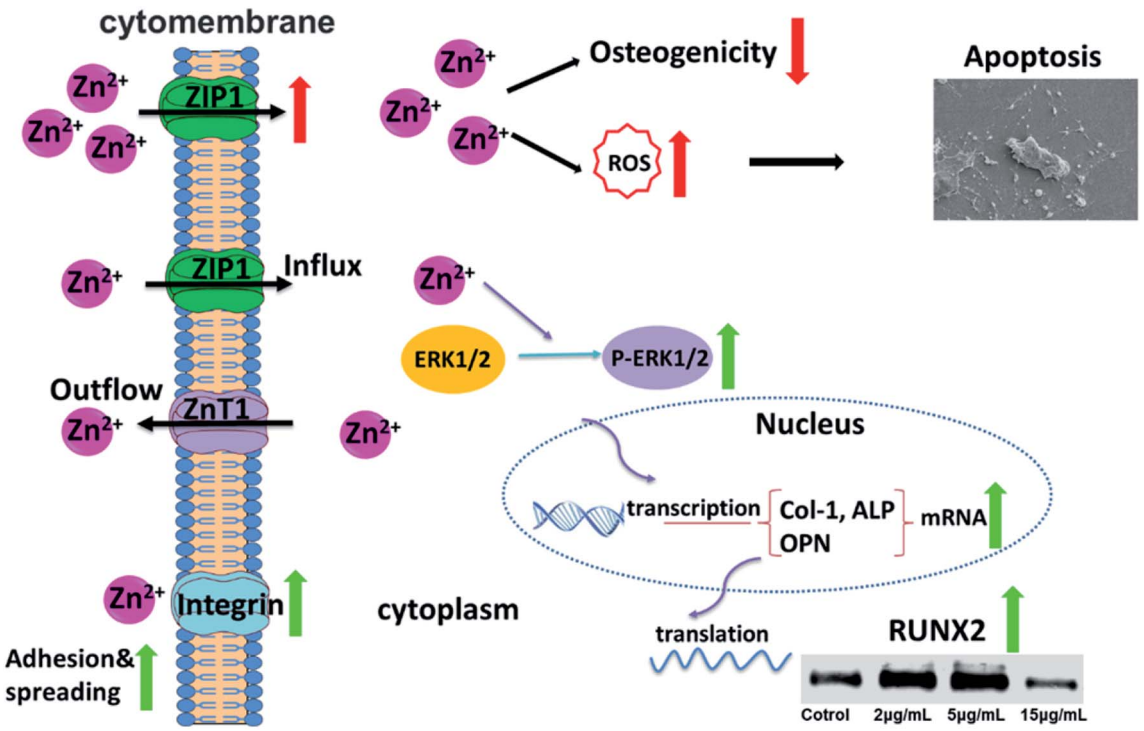

Fig. 7 Underlying mechanism on the double-edged effects of Zn^{2+} microenvironments on rBMSCs.

studies have validated that the cytotoxicity and bactericidal effect of Nano-ZnO are also closely related to its release of high concentration Zn^{2+} and ROS generation.[54,55] In order to control the cytotoxicity of Nano-ZnO, some exploration work has been carried out. For instance, by the covering of PDA and RGDC, the cytocompatibility of Nano-ZnO-loaded titanium can be enhanced through the decrease of both ROS generation and Zn^{2+} release.[41] Nevertheless, the critical concentration of Zn^{2+} microenvironments that induces BMSC apoptosis and the involved mechanism remain unclear so far. Therefore, the current study systematically probed in these problems, and this article may provide a valuable reference for the development of zinc alloys and zinc-doped/Nano-ZnO-loaded materials with superior bifunctionality and biosafety.

3.5 The underlying mechanism on the double-edged effects of Zn^{2+} microenvironments

To sum up, Zn^{2+} microenvironments have "double-edged sword" effects on rBMSCs *via* different regulatory mechanisms. The suitable concentrations of Zn^{2+} (2–5 μg mL^{-1}) can effectively enhance cell adhesion and proliferation of rBMSCs by up-regulating the expression of integrin α1 and integrin β1. More importantly, these optimal Zn^{2+} microenvironments can moderately increase the intracellular Zn^{2+} content by the appropriate promotion of ZIP1 and ZnT1 expression, and can further activate the MAPK/ERK signaling pathway and enhance the expression of osteogenesis-related markers (ALP, Col-1 and OPN), thus inducing the osteogenic differentiation of rBMSCs (Fig. 7). In contrast, the disadvantageous microenvironments with high Zn^{2+} concentration (15 μg mL^{-1}) inhibit cell adhesion and proliferation by down-regulating the expression of integrins. In addition, this kind of Zn^{2+} microenvironments lead to excessive Zn^{2+} inflow into rBMSCs due to over-upregulating the expression of ZIP1. As a result, the excessive intracellular zinc ions not only inhibit osteogenic differentiation of rBMSCs but also induce rBMSCs apoptosis by increased intracellular ROS production (Fig. 7). The underlying mechanism on the double-edged effects of Zn^{2+} microenvironments on BMSCs is clearly illustrated in Fig. 7. The discovery of this mechanism may contribute to amplifying the osteogenic effects of zinc-doped biomaterials and to avoiding their adverse biological influences effectively.

4. Conclusions

Zn^{2+} microenvironments have double-edged effects on BMSCs depending on their diverse concentrations. The appropriate Zn^{2+} microenvironments (2–5 μg mL^{-1}) can not only effectively enhance the initial adhesion and proliferation of rBMSCs but also moderately increase intracellular Zn^{2+} concentration by regulating zinc transportation, and further induce the osteogenic differentiation of rBMSCs by activating MAPK/ERK signaling pathway. By contrast, the excessively high concentration of Zn^{2+} microenvironments (15 μg mL^{-1}) not only reduce the initial adhesion and proliferation of rBMSCs but also inhibit their osteogenic differentiation due to the excessive Zn^{2+} influx and the broken zinc homeostasis. Meanwhile, the overdose of intracellular zinc ions induces rBMSCs apoptosis by facilitating the generation of intracellular ROS.

Conflicts of interest

There is no conflict of interest.

Acknowledgements

The present work was financially supported by grants from the National Natural Science Foundation of China (No. 81873715 and 81572114), the Natural Science Foundation of Shanghai (No. 18441902100) and the Fundamental Research Funds for the Chinese Central Universities (No. 1504219051).

References

1 D. Zhu, I. Cockerill, Y. Su, Z. Zhang, J. Fu, K. W. Lee, J. Ma, C. Okpokwasili, L. Tang, Y. Zheng, Y. X. Qin and Y. Wang, *ACS Appl. Mater. Interfaces*, 2019, **11**, 6809–6819.
2 K. Xiong, J. Zhang, Y. Zhu, L. Chen and J. Ye, *Mater. Sci. Eng., C*, 2019, **105**, 110065.
3 C. Heras, S. Sanchez-Salcedo, D. Lozano, J. Pena, P. Esbrit, M. Vallet-Regi and A. J. Salinas, *Acta Biomater.*, 2019, **89**, 359–371.
4 Y. Li, Y. Han, X. Wang, J. Peng, Y. Xu and J. Chang, *ACS Appl. Mater. Interfaces*, 2017, **9**, 16054–16062.
5 G. Jin, H. Cao, Y. Qiao, F. Meng, H. Zhu and X. Liu, *Colloids Surf., B*, 2014, **117**, 158–165.
6 Y. Su, I. Cockerill, Y. Wang, Y. X. Qin, L. Chang, Y. Zheng and D. Zhu, *Trends Biotechnol.*, 2019, **37**, 428–441.
7 W. Maret, *Adv. Nutr.*, 2013, **4**, 82–91.
8 E. Saino, S. Grandi, E. Quartarone, V. Maliardi, D. Galli, N. Bloise, L. Fassina, M. G. De Angelis, P. Mustarelli, M. Imbriani and L. Visai, *Eur. Cells Mater.*, 2011, **21**, 59–72.
9 H. Hu, W. Zhang, Y. Qiao, X. Jiang, X. Liu and C. Ding, *Acta Biomater.*, 2012, **8**, 904–915.
10 K. Huo, X. Zhang, H. Wang, L. Zhao, X. Liu and P. K. Chu, *Biomaterials*, 2013, **34**, 3467–3478.
11 M. Arakha, J. Roy, P. S. Nayak, B. Mallick and S. Jha, *Free Radicals Biol. Med.*, 2017, **110**, 42–53.
12 C. Chen, W. Bu, H. Ding, Q. Li, D. Wang, H. Bi and D. Guo, *Cell Proliferation*, 2017, **50**, e12339.
13 K. H. Park, Y. Choi, D. S. Yoon, K. M. Lee, D. Kim and J. W. Lee, *Stem Cells Dev.*, 2018, **27**, 1125–1135.
14 E. Fathi and R. Farahzadi, *PLoS One*, 2017, **12**, e0173877.
15 X. Shen, Y. Zhang, P. Ma, L. Sutrisno, Z. Luo, Y. Hu, Y. Yu, B. Tao, C. Li and K. Cai, *Biomaterials*, 2019, **212**, 1–16.
16 A. Krol, P. Pomastowski, K. Rafinska, V. Railean-Plugaru and B. Buszewski, *Adv. Colloid Interface Sci.*, 2017, **249**, 37–52.
17 W. Yuan, B. Li, D. Chen, D. Zhu, Y. Han and Y. Zheng, *ACS Biomater. Sci. Eng.*, 2019, **5**, 487–497.
18 D. S. Brauer, E. Gentleman, D. F. Farrar, M. M. Stevens and R. G. Hill, *Biomed. Mater.*, 2011, **6**, 045007.
19 S. A. James, B. N. Feltis, M. D. de Jonge, M. Sridhar, J. A. Kimpton, M. Altissimo, S. Mayo, C. Zheng,

A. Hastings, D. L. Howard, D. J. Paterson, P. F. Wright, G. F. Moorhead, T. W. Turney and J. Fu, *ACS Nano*, 2013, **7**, 10621–10635.

20 H. M. Davis, P. C. Rafael, E. G. Atkinson, L. R. Brun, A. R. Gortazar, J. Harris, M. Hiasa, S. A. Bolarinwa, T. Yoneda, M. Ivan, A. Bruzzaniti, T. Bellido and L. I. Plotkin, *Aging Cell*, 2017, **16**, 551–563.

21 T. Kambe, T. Tsuji, A. Hashimoto and N. Itsumura, *Physiol. Rev.*, 2015, **95**, 749–784.

22 E. Bafaro, Y. Liu, Y. Xu and R. E. Dempski, *Signal Transduction Targeted Ther.*, 2017, **2**, 1–12.

23 Y. Yu, G. Jin, Y. Xue, D. Wang, X. Liu and J. Sun, *Acta Biomater.*, 2017, **49**, 590–603.

24 Y. Qiao, W. Zhang, P. Tian, F. Meng, H. Zhu, X. Jiang, X. Liu and P. K. Chu, *Biomaterials*, 2014, **35**, 6882–6897.

25 G. Jin, H. Qin, H. Cao, S. Qian, Y. Zhao, X. Peng, X. Zhang, X. Liu and P. K. Chu, *Biomaterials*, 2014, **35**, 7699–7713.

26 S. Vanhatupa, S. Miettinen, P. Pena and C. Baudin, *J. Biomed. Mater. Res., Part B*, 2019, **3**, 1–15.

27 C. Wang, K. Lin, J. Chang and J. Sun, *Biomaterials*, 2013, **34**, 64–77.

28 X. Wu, S. Zheng, Y. Ye, Y. Wu, K. Lin and J. Su, *Biomater. Sci.*, 2018, **6**, 1147–1158.

29 C. Niu, F. Xiao, K. Yuan, X. Hu, W. Lin, R. Ma, X. Zhang and Z. Huang, *Front. Pharmacol.*, 2017, **8**, 626.

30 J. Liu, W. Liu, Y. Lu, H. Tian, C. Duan, L. Lu, G. Gao, X. Wu, X. Wang and H. Yang, *Autophagy*, 2018, **14**, 845–861.

31 H. Xu, C. X. Chen, J. Hu, P. Zhou, P. Zeng, C. H. Cao and J. R. Lu, *Biomaterials*, 2013, **34**, 2731–2737.

32 Q. Zhao, L. Yi, L. Jiang, Y. Ma, H. Lin and J. Dong, *Nanomedicine*, 2019, **16**, 149–161.

33 G. Katarivas Levy, A. Kafri, Y. Ventura, A. Leon, R. Vago, J. Goldman and E. Aghion, *Mater. Lett.*, 2019, **248**, 130–133.

34 E. R. Shearier, P. K. Bowen, W. He, A. Drelich, J. Drelich, J. Goldman and F. Zhao, *ACS Biomater. Sci. Eng.*, 2016, **2**, 634–642.

35 M. Michael and M. Parsons, *Curr. Opin. Cell Biol.*, 2020, **63**, 31–37.

36 Y. Yu, T. Ding and Y. Xue, *J. Mater. Chem.*, 2016, **4**, 801–812.

37 D. Zhu, Y. Su, M. L. Young, J. Ma, Y. Zheng and L. Tang, *ACS Appl. Mater. Interfaces*, 2017, **9**, 27453–27461.

38 S. K. Nethi, N. A. P. Anand, B. Rico-Oller, A. Rodriguez-Dieguez, S. Gomez-Ruiz and C. R. Patra, *Sci. Total Environ.*, 2017, **599–600**, 1263–1274.

39 H. J. Seo, Y. E. Cho, T. Kim, H. I. Shin and I. S. Kwun, *Nutr. Res. Pract.*, 2010, **4**, 356–361.

40 P. E. Petrochenko, Q. Zhang, R. Bayati, S. A. Skoog, K. S. Phillips, G. Kumar, R. J. Narayan and P. L. Goering, *Toxicol. In Vitro*, 2014, **28**, 1144–1152.

41 J. Li, L. Tan, X. Liu, Z. Cui, X. Yang, K. W. K. Yeung, P. K. Chu and S. Wu, *ACS Nano*, 2017, **11**, 11250–11263.

42 H. Kao, C. Chen, Y. Huang, Y. Chu, A. Csík and S. Ding, *Surf. Coating. Technol.*, 2019, **378**, 124998.

43 T. Kimura and T. Kambe, *Int. J. Mol. Sci.*, 2016, **17**, 336.

44 Y. Wang, J. Li, W. Song and J. Yu, *Cell Proliferation*, 2014, **47**, 241–248.

45 Y. Li, C. Ge and R. T. Franceschi, *J. Cell. Physiol.*, 2017, **232**, 2427–2435.

46 M. Bruderer, R. G. Richards, M. Alini and M. J. Stoddart, *Eur. Cells Mater.*, 2014, **28**, 269–286.

47 W. Watjen, H. Haase, M. Biagioli and D. Beyersmann, *Environ. Health Perspect.*, 2002, **110**(suppl 5), 865–867.

48 H. He, Y. Qiao, Q. Zhou, Z. Wang, X. Chen, D. Liu, D. Yin and M. He, *Oxid. Med. Cell. Longevity*, 2019, **2019**, 2340392.

49 B. Zhou, J. Y. Zhang, X. S. Liu, H. Z. Chen, Y. L. Ai, K. Cheng, R. Y. Sun, D. Zhou, J. Han and Q. Wu, *Cell Res.*, 2018, **28**, 1171–1185.

50 L. Fan, J. Wang and C. Ma, *J. Cell. Physiol.*, 2020, **235**, 2857–2865.

51 M. Cierech, J. Wojnarowicz, A. Kolenda, A. Krawczyk-Balska, E. Prochwicz, B. Wozniak, W. Lojkowski and E. Mierzwinska-Nastalska, *Nanomaterials*, 2019, **9**, 1318.

52 Y. Y. Kao, Y. C. Chen, T. J. Cheng, Y. M. Chiung and P. S. Liu, *Toxicol. Sci.*, 2012, **125**, 462–472.

53 X. Zhao, X. Ren, R. Zhu, Z. Luo and B. Ren, *Aquat. Toxicol.*, 2016, **180**, 56–70.

54 W. He, H. K. Kim, W. G. Wamer, D. Melka, J. H. Callahan and J. J. Yin, *J. Am. Chem. Soc.*, 2014, **136**, 750–757.

55 W. Song, J. Zhang, J. Guo, J. Zhang, F. Ding, L. Li and Z. Sun, *Toxicol. Lett.*, 2010, **199**, 389–397.